JOURNAL OF GUIDANCE, CONTROL, AND DYNAMICS
Vol. 17, No. 1, January–February 1994

Optimal Tendon Configuration of a Tendon Control System for a Flexible Structure

Jin Lu*
Odyssey Research Associates, Inc., Ithaca, New York 14850
and
James S. Thorp,† Brian H. Aubert,‡ and Lauran B. Larson§
Cornell University, Ithaca, New York 14853

This paper considers the optimal tendon configuration of a tendon control system for a two-dimensional, eleven-bay truss. With the criterion for optimal tendon configuration being controllability and robustness of the tendon control system, the optimal tendon configuration problem can be formulated as a constrained optimization problem which can be solved using dynamic programming; therefore, a solution to the optimal tendon configuration problem can be obtained efficiently. The robustness of the resulting tendon control system with respect to modeling imperfections is studied.

I. Introduction

THE problem of optimal actuator placement for active vibration suppression of a large flexible space structure (LFSS) has been studied recently.[1-3] A common way to deal with this problem is to formulate it as a constrained optimization problem in which the objective function is the criterion for optimal actuator placement and the constraints reflect the admissibility of actuators and the special configuration of the structure. There are no efficient algorithms for solving the constrained optimization for a general optimal actuator placement problem.

This paper considers the optimal tendon configuration of a tendon control system for a two-dimensional, eleven-bay truss. The concept of tendon control system has been previously explored.[4,5] The objective of our control system is to enhance the damping of the critical modes of the truss using output feedback control. One of the important issues of using noncollocated controllers to enhance the damping of a LFSS is the robustness of the controllers with respect to modeling imperfections. We choose the controllability and robustness of the tendon control system as the criterion for optimal tendon configuration. We will show that with this criterion of optimality, the optimal tendon configuration problem can be formulated as a constrained optimization problem which can be solved using dynamic programming; therefore a solution to the optimal tendon configuration problem can be obtained efficiently.

This paper is organized as follows. In Sec. II, a system description of the two-dimensional, eleven-bay truss is given. In Sec. III, the optimal tendon configuration problem is formulated as a constrained optimization problem. In Sec. IV, a method is presented for solving the constrained optimization problem using dynamic programming. In Sec. V, optimal tendon configurations are determined using the method, and the robustness of the resulting tendon control systems with respect to modeling imperfections is studied.

Received Oct. 3, 1992; revision received March 29, 1993; accepted for publication March 31, 1993.

*Control Systems Engineer.
†Professor, School of Electrical Engineering.
‡Research Associate, School of Civil and Environmental Engineering.
§Student, School of Civil and Environmental Engineering.

II. System Description

In this section, we describe the two-dimensional, eleven-bay truss and its tendon control system.

A. Two-Dimensional, Eleven-Bay Truss

The two-dimensional, eleven-bay truss under consideration is a Vierendeel truss consisting of eleven 83.8×45.7 cm bays suspended from two fixed upper nodes (see Fig. 1). This model is a two-dimensional simplification of an actual three-dimensional truss under two-dimensional and three-dimensional testing at Cornell University.[6] In the model of the idealized structure (as opposed to the imperfect structures obtained by randomly perturbing the structure elements to study the robustness of feedback control schemes), the members are aluminum tube stock with a modulus of elasticity of 68.9 GPa. The members are prismatic and have an outside diameter of 1.37 cm and a wall thickness of 0.22 cm. The structural members are modeled with linear beam-column finite elements,

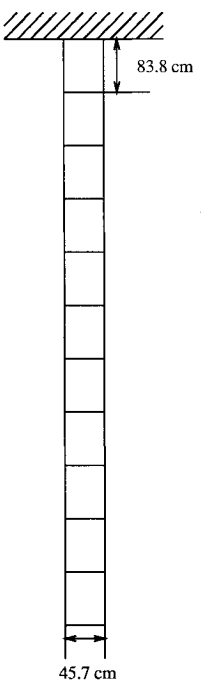

Fig. 1 Eleven-bay truss.

connected at moment-resisting joints. The model mass matrix includes contributions from the members, the connections, and the nodal masses added to the structure to lengthen the structure periods. The masses have been lumped at the nodes. The translational mass at each node is 1.81 kg. The rotational mass is 33.4 kg-cm^2/rad at the interior nodes and 19.6 kg-cm^2/rad at the two bottom nodes. The two-dimensional, eleven-bay truss is modeled via a finite element method as a lumped-parameter, linear time-invariant system:

$$M\ddot{x} + D\dot{x} + Kx = 0 \tag{1}$$

where $x \in \mathfrak{R}^n$ is the vector of nodal displacements, $n = 22 \times 3 = 66$ with 22 being the number of nodes and 3 being the number of displacements of each node. The three displacements of each node include two translational displacements and one rotational displacement. Let the nodal displacements associated with node k be $x_{3(k-1)+1}, x_{3(k-1)+2}, x_{3k}$ (see Fig. 2). Matrices M, D, $K \in \mathfrak{R}^{n\times n}$ are symmetric. Since M is positive and K is nonnegative, there exists a matrix T such that $T^TMT = I$, $T^TKT = \Omega^2 = \text{diag}(\omega_1^2 \cdots \omega_n^2)$. We assume that $0 < \omega_1 < \omega_2 < \cdots < \omega_n$. By transformation $z = T^{-1}x$, the displacement coordinate system (1) is transformed into the modal coordinate system:

$$I\ddot{z} + \bar{D}\dot{z} + \Omega^2 z = 0 \tag{2}$$

where $\bar{D} = T^TDT$. We assume that $\bar{D} = 2\Xi\Omega$, where $\Xi = \text{diag}(\xi_1 \cdots \xi_n)$ with $0 \le \xi_i \ll 1$, $i = 1, \ldots, n$ (small natural damping).

B. Tendon Control System

The tendon control system consists of three subsystems: an actuator system, a sensor system, and a controller.

1. Actuator System

The actuator system includes an electromagnetic actuator (linear motor) mounted on the top end of the truss and a pair of tendons (tension cables) which are mirror images of each other. The tendons are free to slide over the rollers at the end of stiff standoffs at the nodes, allowing both translational and rotational forces to be applied to the nodes. At any moment, at most one tendon is activated (in tension) by the actuator while the other is slack. Because of this fact and the symmetric configuration of the two-dimensional, eleven-bay truss, the pair of tendons can be approximated in effect by an idealized tendon (see Fig. 3) which has the following properties:

1) The idealized tendon is placed as one of the two tendons in Fig. 2.

2) The idealized tendon is stiff and can exert both tensile and compressive forces.

The use of a single tension/compression tendon in place of two tension-only tendons is not exact. However, if a robust active control system is obtained, any small errors in the analytical model will not seriously degrade the performance of the controlled structure. In the sequel, we will only consider the system with the idealized tension/compression tendon as shown in Fig. 3. Once we have the optimal configuration of this idealized tension/compression tendon, the actual tendon configuration is obtained by adding to the one-tendon system a tendon that is the mirror image of the idealized tendon.

Let u be the force exerted through the idealized tendon, then u can be both positive and negative and its effect on the structure is described by the following system

$$M\ddot{x} + D\dot{x} + Kx = Bu \tag{3}$$

where $B \in \mathfrak{R}^n$ is called the control influence vector, whose elements depend on the tendon configuration.

We will neglect the effect of the tendon frequencies on the structure, because the lowest tendon frequencies for the tendon configurations under consideration are much higher than those of the critical modes to be controlled (see Sec. V for more details). We also note that the standoffs are much stiffer than the other members and do not significantly contribute to the structural response. Therefore, we have not explicitly modeled them as structural elements.

2. Sensor System

The sensor system contains a number of accelerometers, say, p accelerometers, for measuring selected nodal accelerations or their linear combinations. The measurement of every accelerometer is conditioned through a low-pass filter, integrated, and amplified to provide a nodal velocity or a linear combination of nodal velocities. Let y_i be the output of the amplifier corresponding to the ith accelerometer, then

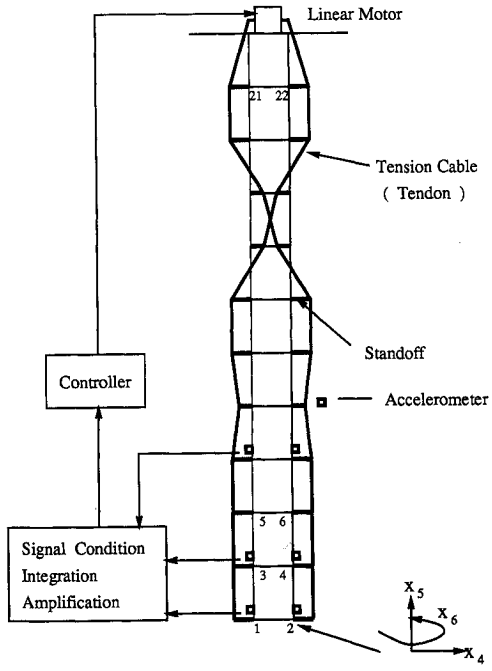

Fig. 2 Tendon control system (numbers are the nodal numbers).

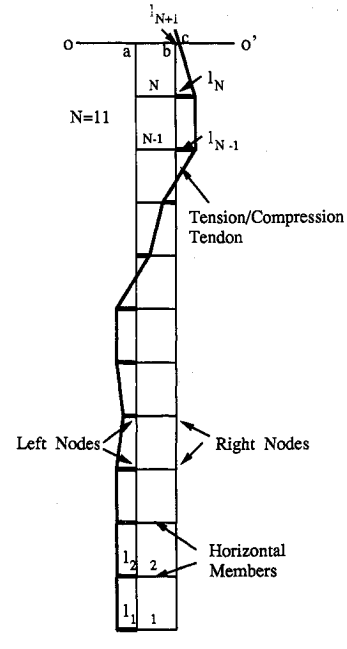

Fig. 3 Idealized tendon system (the tendon can pull and push).

$y_i = c_i \dot{x}$, $i = 1, \ldots, p$ where $c_i \in \mathbb{R}^n$ is a vector whose elements depend on the location of the ith accelerometer. The output vector

$$y = [y_1 \ \cdots \ y_p]^T = [c_1^T \ \cdots \ c_p^T]^T \dot{x} = C\dot{x} \tag{4}$$

is fed into the controller. Matrix $C \in \mathbb{R}^{p \times n}$ is called the measurement matrix.

3. Controller

The controller includes an analog/digital (A/D) converter, a computer, and a digital/analog (D/A) converter. It provides control signals for driving the actuator. The relation between the actuator force u and the output y is

$$u = -Fy \tag{5}$$

where $F \in \mathbb{R}^{l \times p}$ is called an output feedback gain.

III. Problem Formulation

In this section, we formulate the problem of optimal tendon configuration. We first characterize the tendon configuration and then give the criterion for optimal tendon configuration.

A. Characterization of the Tendon Configuration

The configuration of a tendon is uniquely decided by the nodes connected with the tendon, the length of standoffs, and the crossing point c of the tendon to the top line $\overline{oo'}$ (see Fig. 3). For notational clarity, we will use in the following N to denote the number of bays of the truss ($N = 11$) and r to denote the number of displacements associated with each node ($r = 3$).

Define the horizontal members of the truss from bottom to top as member $i = 1, \ldots, N$, respectively. Define the two nodes at the ends of the ith horizontal member as the ith left node and the ith right node, respectively. The ith left node or right node to be connected by a standoff is defined as the ith connected node.

Let e_i, $i = 1, \ldots, N$ and e_{N+1} be defined as

$$e_i = \begin{cases} 1, & \text{if the tendon connects the } i\text{th left node} \\ -1, & \text{if the tendon connects the } i\text{th right node} \end{cases}$$

$$i = 1, \ldots, N$$

$$e_{N+1} = \begin{cases} 1, & \text{if the crossing point } c \text{ is closer to point } a \\ -1, & \text{if the crossing point } c \text{ is closer to point } b \end{cases}$$

Define l_i, $i = 1, \ldots, N$ as variables with the following properties:

1) The variable $|l_i|$ = the length of the standoff connected to the ith connected node.

2) The variable l_i, $i = 1, \ldots, N$ is negative (positive) if it is on the left (right) side of the connected mode.

Define l_{N+1} as a variable with the following properties:

1) The variable $|l_{N+1}| = \min\{\overline{ac}, \overline{bc}\}$ (see Fig. 3).

2) The variable l_{N+1} is negative (positive) if it is on the left (right) side of point a or b, whichever is closer to point c.

We assume that l_i, $i = 1, \ldots, N+1$ are subject to the following constraint

$$-l_m \le l_i \le l_m, \qquad i = 1, \ldots, N+1 \tag{6}$$

for some constant $l_m > 0$.

Let $B = [b_1 \ b_2 \ \cdots \ b_n]^T$. A close examination of the effect of the tendon on the structure reveals that b_i, $i = 1, \ldots, n$ are related to e_i, l_i, $i = 1, \ldots, N+1$ in the following fashion

$$b_j = h_{1,j}(e_1, e_2, l_1, l_2), \qquad j = 1, \ldots, 2r \tag{7}$$

$$b_{2r(i-1)+j} = g_{i,j}(e_{i-1}, e_i, l_{i-1}, l_i) + h_{i,j}(e_i, e_{i+1}, l_i, l_{i+1})$$

$$i = 2, \ldots, N, \qquad j = 1, \ldots, 2r \tag{8}$$

where $g_{i,j}$, $h_{i,j}$ are some nonlinear functions. In other words, how the tendon directly affects the displacements and velocities of nodes $2i-1$ and $2i$ depends only on e_{i-1}, e_i, e_{i+1}, l_{i-1}, l_i, l_{i+1} (or e_i, e_{i+1}, l_i, l_{i+1} when $i = 1$).

B. Criterion for Optimal Tendon Configuration

Let $\Lambda(A, B, C)$ denote the set of the eigenvalues of system

$$A\ddot{x} + B\dot{x} + Cx = 0$$

i.e., $\Lambda(A, B, C) = \{\lambda : |A\lambda^2 + B\lambda + C| = 0\}$. The eigenvalues of the open-loop system (1) [or equivalently, (2)] are

$$\Lambda(M, D, K) = \Lambda(I, \bar{D}, \Omega^2) = \left\{-\xi_i\omega_i \pm j\omega_i\sqrt{1-\xi^2}, \ i = 1, \ldots, n\right\} \tag{9}$$

It is assumed that the first k low-frequency modes of the open-loop system (1) are the critical modes. The eigenvalues associated with the critical modes are $-\xi_i\omega_i \pm j\omega_i\sqrt{1-\xi_i^2}$, $i = 1, \ldots, k$. The objective of the tendon control system is to enhance the damping of the critical modes while keeping the system stable using the output feedback control law (5).

With the transformation $z = T^{-1}x$ used in obtaining Eq. (2) from Eq. (1), system (3) can be written in the modal coordinate form:

$$I\ddot{z} + 2\Xi\Omega\dot{z} + \Omega^2 z = \bar{B}u \tag{10}$$

where $\bar{B} = T^T B$ is defined as a modal control influence vector.

Let $\bar{B} = [\bar{b}_1 \ \cdots \ \bar{b}_n]^T$. The magnitude of $\bar{b}_i$, $i = 1, \ldots, n$ is a measure of controllability of the ith mode, i.e., the effectiveness of the control on the ith mode is proportional to the magnitude of $\bar{b}_i$ ($\bar{b}_i = 0$ implies that mode i is not controllable).[7] Therefore, to make the controller effective on critical modes, it is desirable to have large magnitude of $\bar{b}_i$, $i = 1, \ldots, k$.

On the other hand, when the control scheme (5) is used, the magnitudes of $\bar{b}_i$, $i = 1, \ldots, n$ are measures of the robustness of the stability of the closed-loop modes against structural perturbations. To see this, we substitute $u = -Fy = -FC\dot{x} = -F\bar{C}\dot{z}$, $\bar{C} = CT$ into Eq. (10) to obtain the following closed-loop system:

$$I\ddot{z} + (2\Xi\Omega + \bar{B}F\bar{C})\dot{z} + \Omega^2 z = 0 \tag{11}$$

Assume that $\bar{b}_i \neq 0$, $1 \le i \le n$, which implies that all modes are controllable. Let $\bar{F} = F\bar{C} = [\bar{f}_1 \ \cdots \ \bar{f}_n]$, then we have the following result.

Theorem 1. System (11) is asymptotically stable if $\bar{b}_i\bar{f}_i > 0$, $i = 1, \ldots, n$.

Proof: See Appendix.

We note that there is a result similar to the result of Theorem 1 for a simpler controller under the assumption of zero natural damping.[8]

To guarantee the stability of system (11), we will require that the control feedback gain F in Eq. (5) satisfy the condition $\bar{b}_i\bar{f}_i > 0$, $i = 1, \ldots, n$ for the ideal (nominal) structure. The condition $\bar{b}_i\bar{f}_i > 0$, $i = 1, \ldots, n$, is satisfied if and only if $\bar{f}_i$ has the same sign as $\bar{b}_i$. As a result, the stability of system (11) is robust against the structural perturbations that do not change the sign of $\bar{b}_i$ and $\bar{f}_i$, $i = 1, \ldots, n$ (note that $\bar{B} = T^{-1}B$, $\bar{F} = FCT$ and structural perturbations can change B, C, and T). This suggests that the structure will be likely to remain stable in the presence of structural perturbations if we make $\bar{b}_i, \bar{f}_i$, $i = 1, \ldots, n$ significantly different from zero. Therefore, from the standpoint of robustness, it is desirable to maximize the magnitudes of $\bar{b}_i$, $i = 1, \ldots, n$. Once we have chosen B, we can choose a feedback gain F that achieves the desired damping

improvement under the constraint that $\bar{f}_i$ has the same sign as $\bar{b}_i$ and has a reasonably large magnitude. Because of space limitation, we will not discuss the design of such a feedback gain (it is straightforward using standard output feedback control design methods). Since we are mainly interested in increasing the damping of the critical modes, we only maximize the magnitudes of $\bar{b}_i$, $i=1,\ldots,k$ (k is the number of critical modes).

In summary, it is desirable to maximize the magnitudes of $\bar{b}_i$, $i=1,\ldots,k$ from the standpoint of both controllability and robustness. Since $\bar{b}_i$, $i=1,\ldots,k$ are functions of e_i, l_i, $i=1,\ldots,N+1$, the problem of maximizing the magnitudes of $\bar{b}_i$, $i=1,\ldots,k$ can be formulated as

$$\max_{e_i,l_i,i=1,\ldots,N+1} \sum_{i=1}^{k} \alpha_i |\bar{b}_i(e_i,l_i,\mathrm{i}=1,\ldots,N+1)| \tag{12}$$

where $\alpha_i \geq 0$, $i=1,\ldots,k$ are weighting factors. An appropriate choice of weighting factors must be made to obtain acceptable levels of $\bar{b}_i$, $i=1,\ldots,k$.

Remark 1

Although the optimization problem (12) involves only those $\bar{b}_i$ associated with critical modes, we can include $\bar{b}_i$ associated with a noncritical mode into the set of the $\bar{b}_i$ whose magnitudes are to be maximized, if the magnitude of the $\bar{b}_i$ is too small and the robustness of the noncritical mode is of concern.

Remark 2

Maximizing the magnitudes of $\bar{b}_i$, $i=1,\ldots,k$ enhances the stability robustness of the structure under the control scheme used here. However, large magnitudes of $\bar{b}_i$, $i=1,\ldots,k$ do not guarantee the stability under any perturbations. A limit on the allowable perturbations must be set to guarantee the robustness of the stability. This point will be illustrated by the examples in Sec. V.

Remark 3

In the case of a multi-input system, it is still desirable to have large magnitudes of the components of control influence vector $\bar{B}$. This is because the effectiveness of an actuator on a mode is proportional to the magnitude of the corresponding component of $\bar{B}$; and because even for a multi-input system, a sign change in the components of $\bar{B}$ resulting from perturbations might cause a qualitative change in the controlled system behavior. The large amplitude of a component of $\bar{B}$ makes it possible to retain the sign of the component under perturbations.

IV. Determining the Optimal Tendon Configuration

In this section, we discuss the solution to the optimization problem (12). We first present a method to solve this problem using a dynamic programming and then discuss the numerical aspect of the method.

A. Dynamic Programming

Define $\mathfrak{B}$ as the set of k binary numbers, i.e., $\mathfrak{B}=\{(\beta_1,\ldots,\beta_k):\beta_i\in\{-1,1\}\}$, then the optimization problem (12) is equivalent to the following optimization:

$$\max_{(\beta_1,\ldots,\beta_k)\in\mathfrak{B}} \max_{\substack{e_i,l_i,\\ i=1,\ldots,N+1}} \left(\sum_{i=1}^{k} \beta_i\alpha_i\bar{b}_i(e_i,l_i,l=1,\ldots,N+1)\right) \tag{13}$$

Since k, the number of critical modes, is not very large, the optimization (13) can be solved by the following algorithm:

Algorithm 1:

Step 1: For any sequence $(\beta_1,\ldots,\beta_k)\in\mathfrak{B}$, solve

$$J(\beta_i,\ldots,\beta_k)=\max_{\substack{e_i,l_i,\\ i=1,\ldots,N+1}} \left(\sum_{i=1}^{k} \beta_i\alpha_i\bar{b}_i(e_i,l_i,i=1,\ldots,N+1)\right) \tag{14}$$

Step 2: Find the maximum $J(\beta_i,\ldots,\beta_k)$ over $\mathfrak{B}$ and the associated e_i, l_i, $i=1,\ldots,N+1$.

It is noted that by symmetry of the tendon control system, we have

$$J(\beta_1,\ldots,\beta_k)=J(-\beta_1,\ldots,-\beta_k) \tag{15}$$

and the tendon configurations corresponding to the solutions to the above two optimizations are mirror images of each other. This property leads to the reduction of the number of optimizations in step 1 by half (from 2^k to 2^{k-1}).

The expensive part of the algorithm is solving the optimization problem (14). If l_i, $i=1,\ldots,N+1$ take continuous values, then problem (14) is a mixed nonlinear programming (i.e., nonlinear programming involving integer and continuous variables). In general, a mixed nonlinear programming is complicated and time-consuming.[9] If l_i, $i=1,\ldots,N+1$ take discrete values, then problem (14) is a nonlinear integer programming. A nonlinear integer programming is generally an NP-complete problem, which is also time-consuming. Fortunately, the optimization problem (14) can be transformed into one that can be solved efficiently via dynamical programming.

Let $s_i=[s_{i1}\ \ldots\ s_{in}]$ be the ith row of $\bar{T}^T$. From Eqs. (7) and (8), the ith element of $\bar{B}=T^TB$ is

$$\begin{aligned}\bar{b}_i &= \sum_{j=1}^{n} s_{ij}b_j = \sum_{p=1}^{N}\sum_{q=1}^{2r} s_{i,2r(p-1)+q}\,b_{2r(p-1)+q} \\ &= \sum_{p=1}^{N} f_{i,p}(e_p,e_{p+1},l_p,l_{p+1}), \qquad i=1,\ldots,n\end{aligned} \tag{16}$$

where

$$\begin{aligned}f_{i,p}(e_p,e_{p+1},l_p,l_{p+1}) &= \sum_{q=1}^{2r}\big(s_{i,2r(p-1)+q}h_{p,q}(e_p,e_{p+1},l_p,l_{p+1}) \\ &\quad + s_{i,2rp+q}g_{p+1,q}(e_p,e_{p+1},l_p,l_{p+1})\big), \quad p=1,\ldots,N-1\end{aligned}$$

$$f_{i,N}(e_N,e_{N+1},l_N,l_{N+1})=\sum_{q=1}^{2r} s_{i,2r(N-1)+q}h_{N,q}(e_N,e_{N+1},l_N,l_{N+1})$$

Substituting expression (16) into Eq. (14), we have

$$J(\beta_i,\ldots,\beta_k)=\max_{e_i,l_i,i=1,\ldots,N+1}\left(\sum_{p=1}^{N}\bar{f}_p(e_p,e_{p+1},l_p,l_{p+1})\right) \tag{17}$$

where $\bar{f}_p(e_p,e_{p+1},l_p,l_{p+1}=\Sigma_{i=1}^{k}\beta_i\alpha_i f_{i,p}(e_p,e_{p+1},l_p,l_{p+1})$.

We have rearranged the terms of the objective function in Eq. (14) to obtain Eq. (17). The objective function in Eq. (17) contains N functions, each of which involves only a small subset of the variables. Therefore, optimization (17) can be written as

$$\begin{aligned}J(\beta_i,\ldots,\beta_k)=\max_{e_{N+1},l_{N+1}}\Bigg(\max_{e_N,l_N}\Big\{&\bar{f}_N(e_N,e_{N+1},l_N,l_{N+1}) \\ &+\max_{e_{N-1},l_{N-1}}\Big\{\bar{f}_{N-1}(e_{N-1},e_N,l_{N-1},l_N)+\cdots \\ &+\max_{e_2,l_2}\big\{\bar{f}_2(e_2,e_3,l_2,l_3)+\max_{e_1,l_1}\bar{f}_1(e_1,e_2,l_1,l_2)\big\}\cdots\Big\}\Big\}\Bigg)\end{aligned} \tag{18}$$

Such an optimization problem can be solved by the following dynamic programming in a sequential fashion.[9,10]

Dynamic Programming

Step 1: Solve

$$J_2(e_2,l_2)=\max_{e_1,l_1}\bar{f}_1(e_1,e_2,l_1,l_2) \tag{19}$$

for every pair $(e_2,l_2)\in\{e_2\in\{1,-1\},\ -l_m\leq l_2\leq l_m\}$. Denote the solutions as $e_1^*(e_2,l_2), l_1^*(e_2,l_2)$.

Step 2: For $p=3,\ldots,N+1$, solve

$$J_p(e_p,l_p)=\max_{e_{p-1},l_{p-1}}\left(\bar{f}_{p-1}(e_{p-1},e_p,l_{p-1},l_p)+J_{p-1}(e_{p-1},l_{p-1})\right) \tag{20}$$

for every pair $(e_p,l_p)\in\{e_p\in\{1,-1\},\ -l_m\le l_p\le l_m\}$. Denote the solutions as $e^*_{p-1}(e_p,l_p)$, $l^*_{p-1}(e_p,l_p)$, $p=3,\ldots,N+1$.

Step 3: Determine e^*_{N+1}, l^*_{N+1} such that

$$J=J_{N+1}(e^*_{N+1},l^*_{N+1})=\max_{e_{N+1},l_{N+1}}J_{N+1}(e_{N+1},l_{N+1}) \tag{21}$$

Step 4: For $p=N,\ N-1,\ldots,1$, let $e^*_p=e^*_p(e^*_{p+1},l^*_{p+1})$, $l^*_p=l^*_p(e^*_{p+1},l^*_{p+1})$. Here, $e^*_p(e_{p+1},l_{p+1})$, $l^*_p(e_{p+1},l_{p+1})$, $p=N$, $N-1,\ldots,1$, are solutions to Eqs. (19) and (20) in steps 1 and 2.

The sequence $\{e^*_p,l^*_p,\ p=1,\ldots,N+1\}$ obtained in step 4 is the solution to optimization (17).[9,10]

In practice, e^*_{N+1}, l^*_{N+1} are often prespecified based on other design requirements. In this case, step 3 of the dynamic programming is omitted.

The previous dynamic programming decomposes an optimization problem involving many variables into a series of optimization problems, each of them involves fewer variables. To see the effectiveness of the dynamic programming, we consider the numerical aspect of implementing the dynamic programming.

B. Implementation of the Dynamic Programming

For simplicity, we assume that l_i takes discrete values:

$$l_i\in\mathcal{L}\equiv\{-K\Delta l,\ -(K-1)\Delta l,\ldots\ \Delta l,\ 0,\ \Delta l,\ldots,\ (K-1)\Delta l,\ K\Delta l\}\subset[-l_m,\ l_m] \tag{22}$$

where $\Delta l>0$ is a small increment and integer $K=l_m/\Delta l$. If Δl is sufficiently small, the optimal solution in the discrete case is close to that in the continuous case.

With l_i taking discrete values, the dynamic programming is implemented by creating two matrices P, $J\in\mathcal{R}^{2(2K+1)\times N}$ as follows

$$J=\begin{bmatrix}
J_2(1,-K\Delta l) & J_3(1,-K\Delta l) & \cdots & J_{N+1}(1,-K\Delta l)\\
J_2(1,-(K-1)\Delta l) & J_3(1,-(K-1)\Delta l) & \cdots & J_{N+1}(1,-(K-1)\Delta l)\\
\vdots & \vdots & \cdots & \vdots\\
J_2(1,k\Delta l) & J_3(1,K\Delta l) & \cdots & J_{N+1}(1,K\Delta l)\\
J_2(-1,-K\Delta l) & J_3(-1,-K\Delta l) & \cdots & J_{N+1}(-1,-K\Delta l)\\
J_2(-1,-(K-1)\Delta l) & J_3(-1,-(K-1)\Delta l) & \cdots & J_{N+1}(-1,-(K-1)\Delta l)\\
\vdots & \vdots & \cdots & \vdots\\
J_2(-1,K\Delta l) & J_3(-1,K\Delta l) & \cdots & J_{N+1}(-1,K\Delta l)
\end{bmatrix}$$

$$P=\begin{bmatrix}
(e^*_1(1,-K\Delta l),l^*_1(1,-K\Delta l)) & (e^*_2(1,-K\Delta l),l^*_2(1,-K\Delta l)) & \cdots & (e^*_N(1,-K\Delta l),l^*_N(1,-K\Delta l))\\
(e^*_1(1,-(K-1)\Delta l),l^*_1(1,-(K-1)\Delta l)) & (e^*_2(1,-(K-1)\Delta l),l^*_2(1,-(K-1)\Delta l)) & \cdots & (e^*_N(1,-(K-1)\Delta l),l^*_N(1,-(K-1)\Delta l))\\
\vdots & \vdots & \cdots & \vdots\\
(e^*_1(1,K\Delta l),l^*_1(1,K\Delta l)) & (e^*_2(1,K\Delta l),l^*_2(1,K\Delta l)) & \cdots & (e^*_N(1,K\Delta l),l^*_N(1,K\Delta l))\\
(e^*_1(-1,-K\Delta l),l^*_1(-1,-K\Delta l)) & (e^*_2(-1,-K\Delta l),l^*_2(-1,-K\Delta l)) & \cdots & (e^*_N(-1,-K\Delta l),l^*_N(-1,-K\Delta l))\\
(e^*_1(-1,-(K-1)\Delta l),l^*_1(-1,-(K-1)\Delta l)) & (e^*_2(-1,-(K-1)\Delta l),l^*_2(-1,-(K-1)\Delta l)) & \cdots & (e^*_N(-1,-(K-1)\Delta l),l^*_N(-1,-(K-1)\Delta l))\\
\vdots & \vdots & \cdots & \vdots\\
(e^*_1(-1,K\Delta l),l^*_1(-1,K\Delta l)) & (e^*_2(-1,K\Delta l),l^*_2(-1,K\Delta l)) & \cdots & (e^*_N(-1,K\Delta l),l^*_N(-1,K\Delta l))
\end{bmatrix}$$

Matrix J records $J_p(e_p,l_p)$, $e_p\in\{1,-1\}$, $l_p\in\mathcal{L}$, $p=2,\ldots,N+1$, and matrix P records $e^*_{p-1}(e_p,l_p)$, $l^*_{p-1}(e_p,l_p)$, $p=2,\ldots,N+1$. Both $J_p(e_p,l_p)$ and $e^*_{p-1}(e_p,l_p)$, $l^*_{p-1}(e_p,l_p)$, $p=2,\ldots,N+1$, are obtained in steps 1 and 2 of the dynamic programming.

Once the two matrices are obtained, the optimal choice of e_i, l_i, $i=1,\ldots,N+1$ is readily obtained from the two matrices. For example, suppose that we find

$$J_{N+1}(1,K\Delta l)=\max_{e_{N+1,N+1}}J_{N+1}(e_{N+1},l_{N+1})$$

from matrix J. We then look for $(e^*_N(1,K\Delta l),\ l^*_N(1,K\Delta l))$ from matrix P and let $e^*_N=e^*_N(1,K\Delta l)$ and $l^*_N=l^*_N(1,K\Delta l)$. Suppose

$$e^*_N(1,K\Delta l)=-1,\qquad l^*_N(1,K\Delta l)=-K\Delta l$$

We then look for $e^*_{N-1}(-1,-K\Delta l)$, $l^*_{N-1}(-1,-K\Delta l)$ from matrix P, which are e^*_{N-1} and l^*_{N-1}, respectively. We proceed this way until we find e^*_1 and l^*_1 from matrix P.

To obtain $J_p(e_p,l_p)$ and $e^*_{p-1}(e_p,l_p)$, $l^*_{p-1}(e_p,l_p)$ for fixed e_p and l_p, we need to calculate and compare $2(2K+1)$ numbers

$$\bar{f}_{p-1}(e_{p-1},e_p,l_{p-1},l_p)+J_{p-1}(e_{p-1},l_{p-1})$$

$$e_{p-1}\in\{1,-1\},\ l_{p-1}\in\mathcal{L}$$

Let M be the upper bound to the computational amount needed for calculating a single number $\bar{f}_{p-1}(e_{p-1},e_p,l_{p-1},l_p)+J_{p-1}(e_{p-1},l_{p-1})$ plus making a comparison between two numbers, then the computational amount needed for calculating the $2(2K+1)$ numbers is less than $2(2K+1)M$. Therefore the computational amount needed for creating matrices J and P is less than $2(2K+1)M\times 2(2K+1)N=4(2K+1)^2NM$, where $2(2K+1)N$ is the number of entries in matrix J. As a result, the computational amount needed for solving optimization (17) using the dynamic programming is less than $4(2K+1)^2NM$.

The computational amount for solving the original problem (13) using the dynamic programming is at most $2^{k-1}4(2K+1)^2NM$, where 2^{k-1} is the number of optimizations in step 1 of algorithm 1. If, instead of using the dynamic programming, we directly calculate and compare the objective function in Eq. (12) for all the possible choices of e_i, l_i, $i=1,\ldots,N+1$ to obtain the optimal one (exhaustive method), then the needed computational amount is roughly $(2(2K+1))^{N+1}NM$, where $(2(2K+1))^{N+1}$ is the number of all the possible combination of $\{e_p,l_p,p=1,\ldots,N+1\}$, and NM is roughly the computational amount needed for calculating the objective function in Eq. (12) for fixed $\{e_p,l_p,p=1,\ldots,N+1\}$. For example,

Table 1 Open-loop and closed-loop eigenvalues associated with critical modes

Open-loop	Configuration 1	Configuration 2
$0.0 \pm 3.1i$	$-0.8 \pm 3.2i$	$-0.8 \pm 3.2i$
$0.0 \pm 9.4i$	$-2.2 \pm 9.9i$	$-2.0 \pm 9.9i$
$0.0 \pm 16.0i$	$-2.4 \pm 16.4i$	$-3.1 \pm 16.0i$
$0.0 \pm 22.8i$	$-3.6 \pm 21.9i$	$-2.7 \pm 21.6i$
$0.0 \pm 29.8i$	$-1.9 \pm 29.2i$	$-1.4 \pm 29.2i$
$0.0 \pm 37.0i$	$-2.6 \pm 36.0i$	$-1.8 \pm 36.4i$
$0.0 \pm 44.0i$	$-2.5 \pm 42.3i$	$-2.6 \pm 41.9i$
$0.0 \pm 50.7i$	$-1.7 \pm 48.8i$	$-0.8 \pm 49.7i$
$0.0 \pm 56.6i$	$-0.7 \pm 55.8i$	$-0.1 \pm 56.4i$
$0.0 \pm 61.2i$	$-0.6 \pm 60.5i$	$-0.1 \pm 61.1i$
$0.0 \pm 64.2i$	$-0.2 \pm 63.8i$	$-0.4 \pm 63.9i$

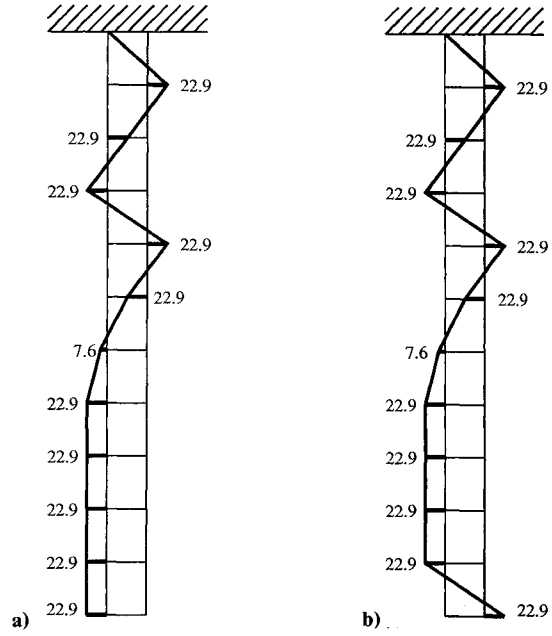

Fig. 4 Two optimal tendon configurations (the numbers are the lengths of standoffs in cm).

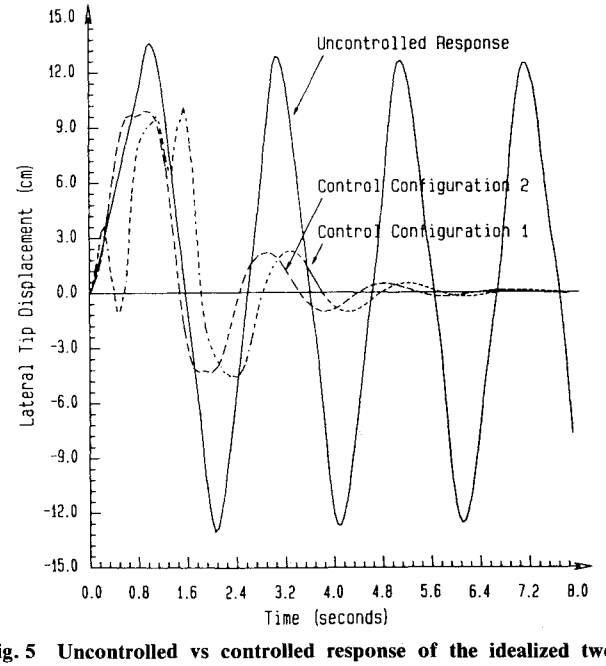

Fig. 5 Uncontrolled vs controlled response of the idealized two-dimensional structure.

let $N = 11$, $K = 10$ and $k = 3$, then the computational amount for the dynamic programming is $2^{k-1}4(2K+1)^2NM = 7056M$ and the computational amount for the exhaustive method is $(2(2K+1))^{N+1}NM = 42^{12} \times 11M$. Therefore, when N is large, the dynamic programming saves a tremendous amount of computation as compared with the exhaustive method.

V. Optimal Tendon Placements of the Eleven-Bay Truss

In this section, two tendon configurations are determined for the eleven-bay truss using the method presented in the previous section. The robustness of the feedback control schemes for both configurations are studied through numerical simulations.

In all numerical simulations described here, we neglect any inherent passive damping of the structure. The critical modes of the idealized (or nominal) structure described in Sec. II are the first eleven low-frequency modes as shown in Table 1. The selected observations are the average horizontal velocities, one at each level, and the rotational velocities of the four lowest nodes. Therefore, $y = C\dot{x} \in \mathcal{R}^{15}$. Once the tendon configuration (or vector B) is determined, feedback gains are calculated so that the critical modes of the closed-loop system have desired damping while the closed-loop system is stable.

The tendon configuration is characterized by e_i, l_i, $i = 1, \ldots, 12$. The lengths of standoffs l_i, $i = 1, \ldots, 11$ are confined between $[-22.9, 22.9]$ cm and take discrete values

$$\{-22.9,\ -15.2,\ -7.6,\ 0.0,\ 7.6,\ 15.2,\ 22.9\}\ \text{cm}$$

and e_{12}, l_{12} are prespecified as $e_{12} = 1$, $l_{12} = 0$.

The following two configurations are considered:

Configuration 1: The tendon configuration is determined so that the lowest-frequency mode is strongly controllable and robustly stable against structural perturbations. This design requirement is formulated as the following optimization:

$$\max_{\substack{e_i, l_i, \\ i=1,\ldots,12}} |\bar{b}_1| = \max_{\substack{e_i, l_i, \\ i=1,\ldots,12}} \bar{b}_1 \tag{23}$$

Configuration 2: The tendon configuration is determined so that the two lowest-frequency critical modes are strongly controllable and robustly stable against structural perturbations. This design requirement is formulated as the following optimization:

$$\max_{\substack{e_i, l_i, \\ i=1,\ldots,12}} \sum_{i=1}^{2} \alpha_i |\bar{b}_i| \tag{24}$$

where $\alpha_i = 1$, $i = 1, 2$.

The optimal tendon configurations satisfying the preceding requirements are determined for the idealized structure using the dynamic programming. The resulting optimal tendon configurations are shown in Fig. 4, and the entries of the corresponding modal control influence vectors associated with the critical modes are listed in Table 2. We note that we do not consider optimization of the $\bar{b}_i$ associated with all critical modes, because the second tendon configuration gives satisfactory magnitudes of all $\bar{b}_i$.

Feedback gains are determined for the two tendon configurations so that the critical modes of the corresponding closed-loop systems have desired damping. As mentioned early, to make the control system robustly stable, feedback gains are chosen under the constraint that $\bar{f}_i$ has the same sign as $\bar{b}_i$ and has a reasonably large magnitude. The eigenvalues associated with the critical modes of the two closed-loop systems are listed in Table 1. Figure 5 shows the dynamic responses of lateral tip displacement of both closed-loop systems to an excitation. The excitation is a lateral impact load applied at a lower

Table 2 Entries of modal control influence vectors $\bar{B}$ associated with the critical modes

	$\bar{b}_1$	$\bar{b}_2$	$\bar{b}_3$	$\bar{b}_4$	$\bar{b}_5$	$\bar{b}_6$	$\bar{b}_7$	$\bar{b}_8$	$\bar{b}_9$	$\bar{b}_{10}$	$\bar{b}_{11}$
Configuration 1	929	−121	1664	−4973	−3201	−8207	−24410	−18399	5248	13428	−15222
Configuration 2	815	841	4161	−9266	2741	−1521	−31810	−11653	10573	17217	−13254

Table 3 Results of transient dynamic analyses with the active controls applied to the perturbed structures

Series	Nodal imperfection (cm)	% of trials stable	
		Configuration 1	Configuration 2
1	±0.0	85	100
2	±1.3	55	100
3	±2.5	15	95
4	±5.1	5	55

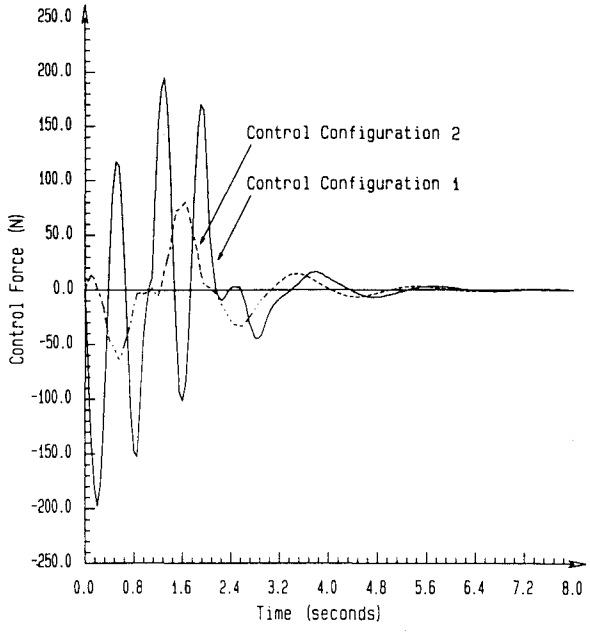

Fig. 6 Control forces for the idealized structure, configuration 1 vs configuration 2.

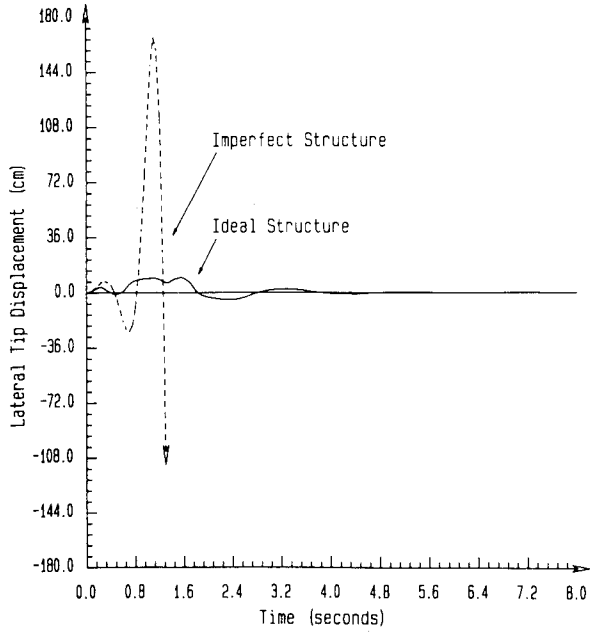

Fig. 7 Typical destabilization of a low-frequency mode for a perturbed structure, control 1.

tip node, with a 22.2 N magnitude, for $t = 1.1$ s. The responses are compared to the response of the uncontrolled structure to the same excitation. Both feedback controls provide acceptable active damping of the excitation. The control forces for the two different configurations are shown in Fig. 6. Although the controllability of the first configuration is optimized with respect to the first mode, the overall control force of the second controller is significantly lower, indicating that the controllability of the second configuration over the other controlled modes is better (therefore, it is more effective in providing damping to the other controlled modes). Specifically, the small magnitude of the second entry in the modal control influence vector of the first configuration results in relatively large control force associated with the second mode. The second mode periodicity is clearly seen in Fig. 6 in the trace of the control force of the first configuration.

We note that for configuration 1, because of the small magnitude of the second entry of the modal control influence vector, it is expected that small structural perturbation tends to destabilize the second-lowest frequency mode by changing the sign of the second entry of the modal control influence vector. For configuration 2, the entries of the modal control influence vector associated with the critical modes are balanced in their magnitudes, therefore it is expected that the critical modes of the closed-loop system are robustly stable against small structural perturbations.

We mentioned in Sec. II that the effect of the tendon frequencies on the structure are neglected, because the lowest tendon frequencies for the tendon configurations under consideration are much higher than those of the critical modes to be controlled. Indeed, the lowest tendon frequencies for configurations 1 and 2 are 35.1 and 46.8 Hz, respectively (the highest critical frequency is 10.2 Hz).

To study the robustness of the feedback control schemes, four series of twenty transient analyses with random structural perturbations have been run for each tendon configuration. Three types of structural perturbations have been introduced in the model. The perturbed quantities are selected to simulate the model uncertainty caused by using nominal structure properties for control design without first taking into account fabrication tolerances and variations in mass and stiffness properties of the actual structure. To simulate the variation between the nominal and real stiffness of the structure members, the cross-sectional areas and moment of inertia values of the members are randomly varied in the range of ±10% in all four series of the analysis. The mass variations between the model and the actual frame are expected to be less than the variations in stiffnesses, so a range of ±5% is used in all four series of the analysis. To simulate the differences between the model and the real structure due to fabrication tolerances, four ranges of random nodal perturbations have been selected. The nodal coordinates are randomly varied within the ranges of ±0.0, ±1.3, ±2.5, and ±5.1 cm, respectively, for the four series of analyses. The random variation of the structural properties for each analysis is taken from a uniformly distributed sample within the range for the appropriate series. The ranges of imperfections are selected to encompass imperfections that might realistically be expected in fabrication of a physical model or prototype.

The results of the transient dynamic analyses of the imperfect structures with the two tendon configurations are shown in Table 3. The percentages represent the simulations which did not destabilize the system. The majority of the unstable responses associated with the first tendon configuration occur when the second-lowest frequency mode is destabilized by the controller because of the sign change of the second entry of the

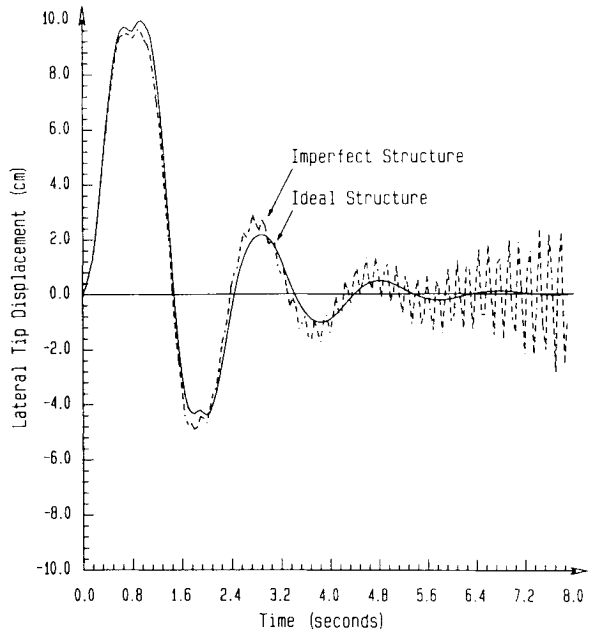

Fig. 8 Typical destabilization of a high-frequency mode for a perturbed structure, control 2.

modal control influence vector. A plot of a lateral tip placement of this type of instability is shown in Fig. 7. The second tendon configuration does not destabilize any low-frequency modes. Some unstable responses of the first controller and all of the unstable responses of the second controller occur when a high-frequency mode, which is not initially supposed to be actively damped, becomes excited by the control forces. A plot of lateral tip placement of this type of instability is shown in Fig. 8. From Table 3, it is obvious that the first tendon configuration is too sensitive to structural perturbations, while the second tendon configuration is fairly robust against structural perturbations.

VI. Conclusion

This paper has discussed the optimal tendon configuration of a tendon control system for a two-dimensional, eleven-bay truss. We have shown that with the criterion for optimal tendon configuration being the controllability and robustness of the tendon control system, the optimal tendon configuration problem can be formulated as a constrained optimization problem which can be solved using dynamic programming; therefore, a solution to the optimal tendon configuration problem can be obtained efficiently. Comparison of the feedback controllers associated with two different optimal tendon configurations demonstrated the effectiveness of this technique.

Appendix: Proof of Theorem 1

Consider the function

$$L(z,\dot{z}) = z^T Q z + \dot{z}^T R \dot{z} \tag{A1}$$

We will show that there exist positive definite matrices Q and R such that $L(z,\dot{z})$ is a Lyapunov function for the closed-loop system (11).

Let $R = \text{diag}([r_1,\ldots,r_n])$ where $r_i = \bar{f}_i/\bar{b}_i$ and $Q = R\Omega^2$. Since $\bar{b}_i\bar{f}_i > 0$, $1 \le i \le n$, R and Q are positive definite matrices. Therefore, $L(z,\dot{z}) = z^T Q z + \dot{z}^T R \dot{z} = 0$ if and only if $z = \dot{z} = 0$.

Differentiating both sides of Eq. (A1), we have

$$\begin{aligned}
&\frac{d}{dt}L(z,\dot{z}) \\
&= \dot{z}^T Q z + z^T Q \dot{z} + \ddot{z}^T R \dot{z} + \dot{z}^T R \ddot{z} \\
&= \dot{z}^T Q z + z^T Q \dot{z} + \left(-(2\Xi\Omega + \bar{B}\bar{F})\dot{z} - \Omega^2 z\right)^T R \dot{z} \\
&\quad + \dot{z}^T R\left(-(2\Xi\Omega + \bar{B}\bar{F})\dot{z} - \Omega^2 z\right) \\
&= \dot{z}^T\left(Q - R\Omega^2\right)z + z^T(Q - \Omega^2 R)\dot{z} \\
&\quad - \dot{z}^T\left((2\Xi\Omega + \bar{B}\bar{F})^T R + R(2\Xi\Omega + \bar{B}\bar{F})\right)\dot{z} \\
&= -2\dot{z}^T(2R\Xi\Omega + \bar{F}^T\bar{F})\dot{z} \le 0 \quad (R\bar{B}\bar{F} = \bar{F}^T\bar{F},\ Q = R\Omega^2)
\end{aligned}$$

Therefore, $L(z,\dot{z})$ is a Lyapunov function.

Next, we will show that the set of $(z,\dot{z})$'s that satisfy $(d/dt)L(z,\dot{z}) = 0$ only contains (0, 0). Therefore, by LaSalle's theorem,[11] the closed-loop system (11) is asymptotically stable.

It is easy to see that

$$\frac{d}{dt}L(z,\dot{z}) = -2\dot{z}^T(2R\Xi\Omega + \bar{F}^T\bar{F})\dot{z} = 0 \tag{A2}$$

$\Rightarrow$ ($R\Xi\Omega$ and $\bar{F}^T\bar{F}$ are non-negative symmetric matrices)

$$\dot{z}^T R\Xi\Omega\dot{z} = 0 \quad \text{and} \quad \dot{z}^T\bar{F}^T\bar{F}\dot{z} = 0 \tag{A3}$$

$\Rightarrow$ ($R > 0$, $\Xi \ge 0$ and $\Omega > 0$ are diagonal matrices.)

$$\Xi\Omega\dot{z} = 0 \quad \text{and} \quad \bar{F}\dot{z} = 0 \tag{A4}$$

Substituting Eq. (A4) into the closed-loop system (11), we have

$$\ddot{z} + \Omega^2 z = 0 \tag{A5}$$

The solution to Eq. (A5) is

$$z = \begin{bmatrix} a_1\sin(\omega_1 t + \delta_1) \\ a_2\sin(\omega_2 t + \delta_2) \\ \vdots \\ a_n\sin(\omega_n t + \delta_n) \end{bmatrix} \tag{A6}$$

Substituting Eq. (A6) into $\bar{F}\dot{z} = 0$ [see Eq. (A4)], we have

$$\sum_{i=1}^{n} \bar{f}_i a_i \omega_i \cos(\omega_i t + \delta_i) = 0 \tag{A7}$$

Because $\cos(\omega_i t + \delta_i)$, $i = 1,\ldots,n$ are linearly independent functions (note that $0 < \omega_1 < \omega_2 < \cdots < \omega_n$), Eq. (A7) implies

$$\bar{f}_i a_i \omega_i = 0, \qquad i = 1,\ldots,n \tag{A8}$$

Since $\bar{f}_i \ne 0$ and $\omega_i > 0$, $i = 1,\ldots,n$, Eq. (A8) implies $a_i = 0$, $i = 1,\ldots,n$ or $z = 0$. Therefore, $(d/dt)L(z,\dot{z}) = 0$ implies $z = \dot{z} = 0$.

Acknowledgments

This work has been supported in part by the Air Force Office of Scientific Research under Contract FQ 8671-8800448. Any opinions expressed herein are those of the authors and do not necessarily reflect the views of the sponsors.

References

[1]Kubrusly, C. S., and Malebranche, H., "Sensors and Controllers Location in Distributed System—A Survey," *Automatica,* Vol. 21, No. 2, 1985, pp. 117-128.

[2]DeLorenzo, M. L., "Sensor and Actuator Selection for Large Space Structure Control," *Journal of Guidance, Control, and Dynamics,* Vol. 13, No. 2, 1990, pp. 249-257.

[3]McCasland, W. N., "Fault-Tolerant Sensor and Actuator Selection for Control of Flexible Structures," *Proceedings of the 1989 American*

Control Conference, June 21–23, 1989, pp. 1111–1113.

[4]Roorda, J., "Experiments in Feedback Control of Structures," *Proceedings of the 1st IUTAM Symposium on Structural Control,* North-Holland, Amsterdam, The Netherlands, 1979, pp. 629–661.

[5]Murotsu, Y., Okubo, H., and Terui, F., "Low Control of Large Space Structures by Using a Tendon Control System," *Journal of Guidance, Control, and Dynamics,* Vol. 12, No. 2, 1989, pp. 264–272.

[6]Larson, L. B., Gergely, P., Lu, J., Thorp, J. S., Aubert, B. H., and Abel, J. F., "An Experimental 10-Meter Space Truss with Tendon Control," *Proceedings of the Second Joint Japan/U.S. Conference on Adaptive Structures,* Nagoya, Japan, Nov. 12–14, 1991, pp. 227–241.

[7]Hamdan, A. M. A., and Hayfeh, A. H., "Measure of Modal Controllability and Observability for First- and Second-Order Linear Systems," *Journal of Guidance, Control, and Dynamics,* Vol. 13, No. 3, 1990, pp. 421–428.

[8]Gevarter, W. B., "Basic Relations for Control of Flexible Vehicles," *AIAA Journal,* Vol. 8, No. 4, 1970, pp. 666–672.

[9]Taha, H. A., *Operations Research—An Introduction,* Macmillan, New York, 1982.

[10]Bellman, R. E., *Dynamic Programming,* Princeton Univ. Press, Princeton, NJ, 1957.

[11]Khalil, H. K., *Nonlinear Systems,* Macmillan, New York, 1992, p. 117.